

# Medical Image Registration Based on an Improved Ant Colony Optimization Algorithm

Ting Xun Lin and Herng Hua Chang

Computational Biomedical Engineering Laboratory (CBEL), Department of Engineering Science and Ocean Engineering, National Taiwan University, Daan 10617 Taipei, Taiwan  
Email: herbertchang@ntu.edu.tw

**Abstract**—Image registration is one of the fundamental and essential tasks within image processing. It is the process of determining the correspondence between structures in two images, which are called the template image and the reference image, respectively. The challenge of registration is to find an optimal geometric transformation between corresponding image data. This paper develops a new image registration algorithm that is based on an improved ant colony optimization algorithm. In our approach, the image pixels are treated as the nest of a swarm of ants. The ants are designed to have the ability to forage for the “food” in their memory. Subsequently, the ants deposit pheromone on the pixels, which affect the motion of the ants. The registration process of updating the pheromone, the direction and distance of advancement is repeated until the correlation coefficient between the registered and reference images reaches a maximum. Experimental results indicate that our method accurately transformed the template images into reference images in various scenarios. It is indicated that the proposed method is of potential in a wide variety of image registration applications.

**Index Terms**—ant colony algorithm, image registration, transition probability

## I. INTRODUCTION

Image registration is one of the fundamental and essential tasks within image processing. It is a process of determining the correspondence between structures in two images, which are called the template image and the reference image, respectively. The intention of registration is to find a correspondent function that maps coordinates from the template image onto the reference image. Image registration has been widely used in computer vision, medical imaging, brain mapping, automatic target recognition, and satellite images. In particular, there is an increasing need for the registration of magnetic resonance (MR) images in many academic and clinical applications such as diagnosis, therapy and surgery planning, and tracking of physical deformations (e.g., tumor growth, brain atrophy) [1]-[4].

Existing registration algorithms can be broadly classified into two major categories according to the transformation models. The first category includes linear transformations, such as rotation, scaling, translation, and

other affine transforms [5]. Methods in the second category allow elastic or non-rigid transformations. These transformations are capable of locally warping the template image to align with the reference image. Approximately, non-rigid transformations include: a) radial basis functions (e.g., thin-plate or surface splines, multi-quadratics, and compactly-supported transformations [6]), b) physical continuum models (e.g., optical flow, linear elasticity, viscous fluids [7]), and c) large deformation models (e.g., diffeomorphisms [8]).

Over the past decades, optical flow methods have been used to find small scale deformations in temporal sequences of medical images [9]. The basic assumption of optical flows is based on the principle of intensity conservation between image frames. For image registration, the motion equation of optical flows is numerically approximated in order to achieve stable transformations for the guidance of the displacement. Moreover, an ant colony optimization algorithm is recently designed to develop effective computer aided techniques for planning software projects [10] and solve the problem of multi-constraint of a non-deterministic polynomial-time hard (NP-Hard) problem [11].

The ambition of this paper is in an attempt to develop a new ant colony registration algorithm that makes use of an improved ant colony model associated with adaptive forage. Our image registration framework combines intensity and pheromone information and exploits the advantages of both classes of information. Unlike most existing non-rigid registration methods, we do not need to calculate complex equations such as Navier–Stokes partial differential equations (PDEs) [7]. The philosophy underlying our algorithm is to develop efficient rules to calculate where ants are foraging for food in images. We will demonstrate the effectiveness of this new registration algorithm on a wide variety of medical images.

## II. REVIEW OF ANT COLONY SYSTEM

Swarm intelligence research originates from the simulation of real ants foraging for food. Ants are able to find the shortest path between the nest and a food source on their way back from the food source based on an attracting substance called *pheromone*. As shown in Fig. 1, the shortest path is considered with the greatest density of pheromone and the ants tend to follow the path with higher pheromone concentration. Dorigo and his partners

Manuscript received November 25, 2015; revised January 25, 2016.

[12] were the first to apply this idea to the traveling salesman problem. This algorithm is referred to as the ant colony algorithm (ACA), which has achieved widespread success in solving different optimization problems, such as the vehicle routing problem, the machine tool tardiness problem and the multiple objective just-in-time (JIT) sequencing problems. Below, we describe the ant colony system in detail.

#### A. Ant System

An ant system is based on the foraging behavior of ants that was first introduced by Dorigo *et al.* [12] and

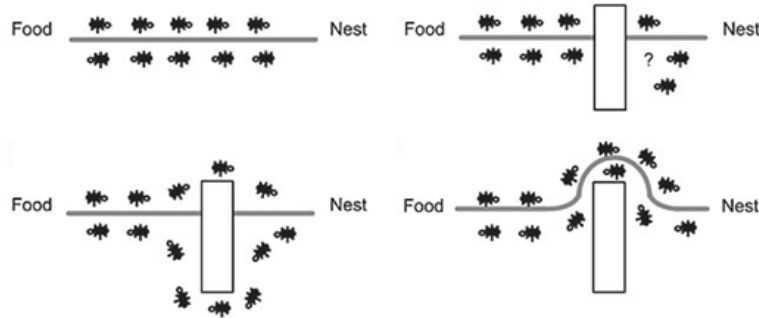


Figure 1. Ants' behavior in forging for food [14]. When the ant faces an obstacle, there is an equal probability for every ant to choose the up or down path. As the up trail is shorter than the down one, it requires less travel time, which results in a higher level of pheromone. This leads to more ants taking the up path and a higher pheromone trail.

In an ant system, ants work as follows. Each ant generates a complete tour by choosing the nodes according to a probabilistic state transition rule: ants prefer to move to nodes which are connected by short paths with a high amount of pheromone [15]. Once all ants have completed their tours a global pheromone updating rule (global updating rule, for short) is applied. A fraction of the pheromone evaporates on all paths and paths that are not refreshed become less desirable. Subsequently, each ant deposits an amount of pheromone on paths which belong to its tour in proportion to how short its tour is. In other words, paths that are composed of more short tours receive a greater amount of pheromone. The process is then iterated.

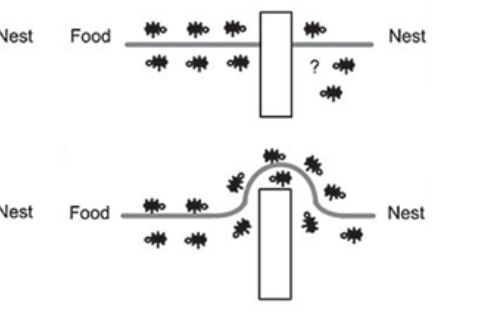
The state transition rule used by the ant system [16], which is also called the random-proportional rule, is defined as

$$p_{ij} = \begin{cases} \frac{[\tau_{ij}]^\alpha [\eta_{ij}]^\beta}{\sum_{h \in \Omega} [\tau_{ih}]^\alpha [\eta_{ih}]^\beta} & \text{if } j \in \Omega \\ 0 & \text{otherwise} \end{cases}. \quad (1)$$

where  $\tau_{ij}$  is the intensity of pheromone between nodes  $i$  and  $j$ ,  $\eta_{ij}$  is the visibility of node  $j$  from node  $i$ ,  $\Omega$  is the set of unvisited nodes,  $\alpha$  and  $\beta$  are two parameters for balancing between  $\tau$  and  $\eta$ . In (1) the pheromone is multiplied by the corresponding heuristic value so that it favors the choice of paths which are shorter and have a greater amount of pheromone. In an ant system, every ant deposits a certain amount of pheromone at the end of each iteration using

$$\text{Pheromone} = \frac{1}{L_k} \quad (2)$$

further formalized as a new meta-heuristic by Dorigo and DiCaro [13]. It is based on the principle of using quite simple communication mechanisms in such a way that an ant group is able to find the shortest path between any two points as shown in Fig. 1. During their trips the chemical trail "pheromone" left on the ground. The role of this chemical trail is to guide the other ants towards the target point with the path chosen according to the quantity of pheromone. Furthermore, this chemical substance has a decreasing action over time and its quantity is proportional to the number of ants on the trail.



where  $L_k$  is the cost of the tour (i.e., path) completed by the ant. After the deposition is accomplished, the pheromone level on every path is decreased using

$$\tau_{ij}(t+1) = (1 - \rho) \times \tau_{ij}(t) \quad (3)$$

where the constant  $\rho$  ( $0 \leq \rho \leq 1$ ) represents the coefficient of decay that is determined at the beginning of the algorithm and  $t$  represents the time step variable.

#### B. Ant Colony System

The ant colony system (ACS) differs from the previous ant system in three main aspects [13]. First, the state transition rule provides a direct way to balance between exploration of a new path and exploitation of an accumulated knowledge about the problem. Second, the global updating rule is applied only to paths that belong to the best ant tour. Last, while ants are constructing a solution a local pheromone updating rule (local updating rule, for short) is applied correspondingly. The pheromone updating rules are designed so that they tend to give more pheromone to paths which should be visited by ants.

Informally, the ACS works as follows [14], [17]: ants are initially positioned on distributed nodes. Each ant builds a tour by repeatedly applying a stochastic greedy rule, which is also known as the state transition rule. While constructing its tour, an ant also modifies the amount of pheromone on the visited paths by applying the local updating rule. Once all ants have terminated their tours, the amount of pheromone on paths is modified again by applying the global updating rule. As was the case in the ant system, ants are guided in building their tours by both heuristic information (they prefer to

choose short paths) and pheromone information. In the following, the state transition rule, the global updating rule, and the local updating rule are discussed.

In ACS, the state transition rule is modified to allow for explicit exploration as [12]:

$$j = \begin{cases} \operatorname{argmax}_{j \in \Omega} \{\tau_{ij} \times \eta_{ij}^\beta\}, & \text{if } q \leq q_0 \\ J, & \text{otherwise} \end{cases} \quad (4)$$

where  $q_0$  is a controlling parameter for the exploration that is assigned at the preprocessing level with  $0 \leq q_0 \leq 1$ ,  $q$  is a uniformly distributed random number determined at each move (i.e., transition from node  $i$  to node  $j$ ),  $J$  is the previous probability distribution function given in (1). If  $q \leq q_0$ , the best node is chosen through exploitation; otherwise, a node is chosen according to biased exploration using (1).

For global updating, only the pheromone on the globally best path (GBP) is updated by increasing the pheromone level using [12]:

$$\tau_{ij}(t+1) = (1 - \sigma) \times \tau_{ij}(t) + \frac{\sigma}{L_{GBP}} \quad (5)$$

where  $\sigma$  is a balancing parameter similar to  $\rho$  in (3). For local updating, the pheromone level of a node is modified before visiting next nodes in a tour using

$$\tau_{ij} = (1 - \varphi) \times \tau_{ij} + \varphi \tau_0 \quad (6)$$

where  $\varphi$  ( $0 < \varphi \leq 1$ ) is the local pheromone concentration coefficient and  $\tau_0$  is the initial value of the pheromone.

### III. ANT REGISTRATION ALGORITHM

The proposed ant colony algorithm for medical image registration utilizes a number of ants moving on a 2-D image to construct a pheromone matrix, which represents the path information at each pixel location of the image. Furthermore, the movements of the ants are guided by the local variation of the image intensity values. Our approach starts from the initialization process followed by the construction process and the update process as shown in Fig. 2. Each of these processes is described in detail as follows.

#### A. Initialization Process

Initially, there are  $M \times N$  ants that are uniformly assigned on the input image  $I$ , which has a corresponding dimension of  $M \times N$ . Each pixel is then viewed as a node and the initial value of the pheromone matrix  $\tau_0$  is set to a constant  $\tau_{init}$ . Now, the challenge is to define what kind of food each ant needs through the use of the previously described ant colony system for image registration. In our approach, the food is represented by the intensity difference between two medical images using

$$I_{diff}^{(n)}(l, m) = I_R(l, m) - I_T^{(n)}(l, m) \quad (7)$$

where  $I_R(l, m)$  is the intensity value of node  $(l, m)$  on the reference image,  $I_T^{(n)}(l, m)$  is the intensity value of node  $(l, m)$  on the template image at the  $n^{th}$  iteration, and  $I_{diff}^{(n)}$  is the difference image at the  $n^{th}$  iteration. If  $I_{diff}^{(n)}$  is

negative, which means that the intensity at node  $(l, m)$  on the template image is larger than that on the reference image, the ant on that node will search for lower intensities around the neighbors as food. On the other hand, if  $I_{diff}^{(n)} \geq 0$ , the ant will search for larger intensity values in the proximity of node  $(l, m)$ .

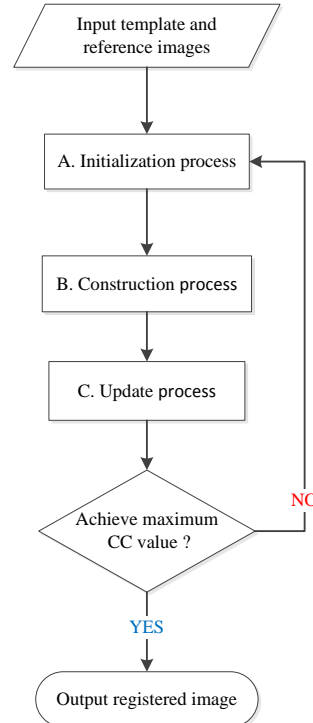


Figure 2. Flow chart of the proposed image registration algorithm.

#### B. Construction Process

After defining the ant's food, the remaining issue is to determine a transition probability function for geometric transformation. In our approach, at the  $n^{th}$  construction step, an ant moves on the path from node  $(l, m)$  to its neighboring node  $(i, j)$  and returns to  $(l, m)$  according to a transition probability function defined as

$$p_{(i,j)}^{(n)}(l, m) = \frac{(\tau^{(n)}(i, j))^\alpha (\eta^{(n)}(i, j))^\beta}{\sum_{(i,j) \in \Omega_{(l,m)}} (\tau^{(n)}(i, j))^\alpha (\eta^{(n)}(i, j))^\beta} \quad (8)$$

where  $\tau^{(n)}(i, j)$  is the pheromone value of node  $(i, j)$ ,  $\Omega_{(l,m)}$  is the neighboring nodes of node  $(l, m)$ ,  $\eta^{(n)}(i, j)$  represents the intensity information at node  $(i, j)$ , and  $n$  is the iteration number. In (8), the constant parameters  $\alpha$  and  $\beta$  represent the influence of the pheromone matrix and the visibility matrix, respectively.

Subsequently, the moving direction of an ant is selected from one of its neighboring coordinates that has the highest probability based on (8). After the direction is decided, the distance of advancement is computed in accordance with the searching of food in (7) using

$$\begin{cases} D_x^{(n)}(l, m) = |r(I_{diff}^{(n)})(T_x^{(n)}(l, m))| \\ D_y^{(n)}(l, m) = |r(I_{diff}^{(n)})(T_y^{(n)}(l, m))| \end{cases} \quad (9)$$

where  $T_x^{(n)}(l, m)$  is the gradient of the registered template image in the  $x$  direction at the  $n^{th}$  iteration,  $T_y^{(n)}(l, m)$  is the gradient of the registered template image in the  $y$  direction at the  $n^{th}$  iteration, and the constant  $r$

represents the scale of the advancing distances  $D_x^{(n)}(l, m)$  and  $D_y^{(n)}(l, m)$  in the  $x$ - and  $y$ -axis, respectively.



Figure 3. Registration of a phantom image and a Lena image. (a) Oval-like to c-shaped image with dimension  $180 \times 150$ . (b) Lena image with dimension  $180 \times 150$ . First column: template images, second column: reference images, third column: registered images, top right panel: intensity difference between registered and reference images, bottom right panel: deformation grid map of Lena.

### C. Update Process

The remaining issue is the update of the pheromone that is carried out after the movement of all ants using

$$\tau^{(n+1)} = e^{-\rho} \times \tau^{(n)} + \tau_{init} \quad (10)$$

where the constant  $\rho$  ( $0 \leq \rho \leq 1$ ) is the coefficient of decay determined at the beginning of the algorithm.

## IV. RESULTS

To evaluate the performance of our improved ant colony algorithm for image registration, a wide variety of images with various scenarios were adopted. We randomly shrank, enlarged, or distorted the images for the experiments. To quantitatively analyse the accuracy of the proposed algorithm, the sum of squared difference (SSD) and the correlation coefficient (CC) between the deformed template image and the reference image were used as given in the following [18]:

$$SSD = \sum \sum \frac{\|A(x,y) - B(x,y)\|^2}{N} \quad (11)$$

$$CC = \frac{\sum \sum (A(x,y) - \bar{A}(x,y)) \sum \sum (B(x,y) - \bar{B}(x,y))}{\sqrt{\sum \sum (A(x,y) - \bar{A}(x,y))^2 \sum \sum (B(x,y) - \bar{B}(x,y))^2}} \quad (12)$$

where  $A(x, y)$  and  $B(x, y)$  represent the intensities of images  $A$  and  $B$  at  $(x, y)$ ,  $\|\cdot\|$  represents the Euclidean norm,  $N$  represents the total pixel number,  $\bar{A}(x, y)$  and  $\bar{B}(x, y)$  represent the average intensities in images  $A$  and  $B$ , respectively.

In Fig. 3(a), we show the registration from an oval-like object to a c-shaped structure using the proposed algorithm. Fig. 3(b) shows that a distorted Lena image was effectively registered and recovered back to a normal

image. We show, in Fig. 4, two examples of registering brain magnetic resonance (MR) images associated with the deformation grid map and the difference image. Finally, in Fig. 5, we show visual registration results of a knee MR image. Table I summarizes the SSD and CC scores of the experiments in Figs. 3 to 5. Obviously, dramatically smaller SSD values and higher CC values were obtained after registration using our method.

TABLE I. QUANTITATIVE ANALYSIS OF THE REGISTRATION RESULTS.

Experiment	SSD		CC	
	Initial	Final	Initial	Final
Fig. 3(a)	0.1155	$2.2617 \times 10^{-4}$	0.4296	0.9848
Fig. 3(b)	0.0017	$1.1615 \times 10^{-5}$	0.7414	0.9931
Fig. 4(a)	0.0012	$5.0369 \times 10^{-5}$	0.9325	0.9930
Fig. 4(b)	0.0008	$1.4577 \times 10^{-5}$	0.9633	0.9991
Fig. 5	0.0031	$1.2895 \times 10^{-4}$	0.8487	0.9930

## V. CONCLUSION

In summary, we have developed a new algorithm for image registration that is based on an improved ant colony optimization model. The proposed approach used simulation of ants foraging for food as the direction of deformation to guide the transformation. Our registration algorithm was extensively evaluated by a number of images with different scenarios. Experimental results indicated that the proposed algorithm achieved high accuracy based on the SSD and CC scores. We believe that this new framework is of potential in a wide variety of image registration applications.

#### ACKNOWLEDGMENT

This work was supported in part by the National Taiwan University under Research Grant No. NTU-CDP-

103R7889 and the Ministry of Science and Technology of Taiwan under contact no. MOST 104-2221-E-002-095.

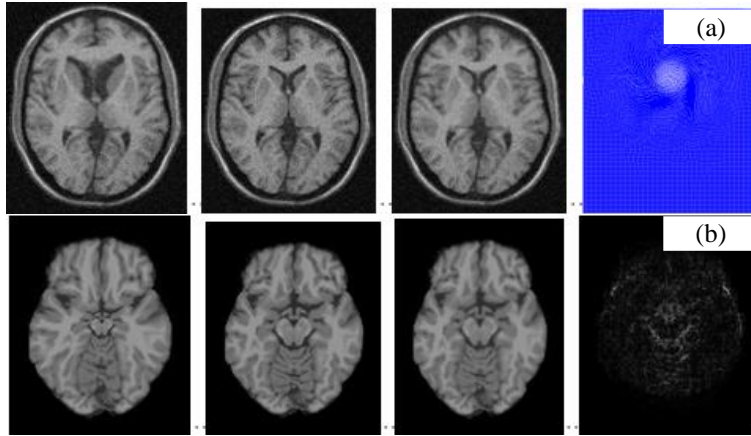


Figure 4. Registration of a brain image and a skull stripped brain image. (a) Brain image with dimension  $217 \times 181$ . (b) Skull stripped brain image with dimension  $217 \times 181$ . First column: template images, second column: reference images, third column: registered images, top right panel: deformation grid map, bottom right panel: intensity difference image.

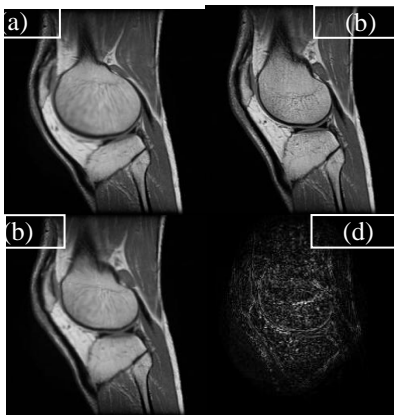


Figure 5. Registration of a knee MR image with dimension  $250 \times 249$ .  
 (a) Template image. (b) Reference image. (c) Registered image. (d) Intensity difference image between the reference and the registered images.

#### REFERENCES

- [1] C. Studholme, C. Drapaca, and V. Cardenas, "Intensity robust viscous fluid deformation based morphometry using regionally adapted mutual information," *Engineering in Medicine and Biology Society*, vol. 1, pp. 470-473, 2005.
- [2] X. Xu and R. D. Dony, "Fast fluid registration using inverse filtering for non-rigid image registration," *Biomedical Imaging: Nano to Macro*, pp. 470-473, 2006.
- [3] S. Tokuhisa and K. Kaneko, "Automatic parameter regulation for CT/MRA viscous fluid registration," in *TENCON 2010 - 2010 IEEE Region 10 Conference*, 2010, pp. 216-221.
- [4] X. Lu, S. Zhang, H. Su, and Y. Chen, "Mutual information-based multimodal image registration using a novel joint histogram estimation," *Computerized Medical Imaging and Graphics*, vol. 32, pp. 202-209, 2008.
- [5] C. H. Chen, L. F. Pau, and P. S. P. Wang, *Handbook of Pattern Recognition and Computer Vision*, World Scientific, 2010.
- [6] A. A. Goshtasby, "2-D and 3-D image registration: for medical, remote sensing, and industrial applications," John Wiley & Sons, 2005.
- [7] M. Holden, "A Review of Geometric Transformations for Nonrigid Body Registration," *Medical Imaging*, vol. 27, pp. 111-128, 2008.
- [8] R. Bowen and J.-R. Chazottes, Equilibrium states and the ergodic theory of Anosov diffeomorphisms vol. 470: Springer, 1975.
- [9] J. P. Thirion, "Image matching as a diffusion process: an analogy with Maxwell's demons," *Medical Image Analysis*, vol. 2, pp. 243-260, 1998.
- [10] H. Wang, Z. Shi, A. Ge, and C. Yu, "An optimized ant colony algorithm based on the gradual changing orientation factor for multi-constraint QoS routing," *Computer Communications*, vol. 32, pp. 586-593, 2009.
- [11] W. N. Chen and J. Zhang, "Ant colony optimization for software project scheduling and staffing with an event-based scheduler," *Software Engineering*, vol. 39, pp. 1-17, 2013.
- [12] M. Dorigo and L. M. Gambardella, "Ant colonies for the travelling salesman problem," *BioSystems*, vol. 43, pp. 73-81, 1997.
- [13] M. Dorigo, G. Caro, and L. Gambardella, "Ant algorithms for discrete optimization," *Artificial Life*, vol. 5, pp. 137-172, 1999.
- [14] M. Perretto and H. S. Lopes, "Reconstruction of phylogenetic trees using the ant colony optimization paradigm," *Genetics and Molecular Research*, vol. 4, pp. 581-589, 2005.
- [15] J. Tian and L. Chen, "Depth image up-sampling using ant colony optimization," in *Pattern Recognition (ICPR)*, 2012, pp. 3795-3798.
- [16] M. G. Cinsikici and D. Aydin, "Detection of blood vessels in ophthalmoscope images using MF/ant (matched filter/ant colony) algorithm," *Computer methods and programs in biomedicine*, vol. 96, pp. 85-95, 2009.
- [17] A. Shi, F. C. Huang, Y. Pan, and L. Z. Xu, "Image registration using ant colony and particle swarm hybrid algorithm based on wavelet transform," *Machine Vision, ICMV '09. Second International Conference* (pp. 41-45), 2009.
- [18] L. Tsai and H. H. Chang, "An incompressible fluid flow model with mutual information for MR image registration," in *IS&T/SPIE Electronic Imaging*, 2013, pp. 86610T-86610T-8.

**Ting-Xun Lin** received his M.S. in 2015 from the Department of Engineering Science and Ocean Engineering at National Taiwan University, Taipei, Taiwan. He was formerly a graduate student in the Computational Biomedical Laboratory (CBEL) directed by Professor Herng-Hua Chang in the Department of Engineering Science and Ocean Engineering at National Taiwan University. His research interests include ant colony optimization system, medical image registration, and computational neuroscience.



**Herng-Hua Chang** received his Ph.D. in biomedical engineering in 2006 from the University of California at Los Angeles (UCLA). He was formerly a postdoctoral scholar with the Laboratory of Neuro Imaging (LONI) and a member of the Center for Computational Biology (CCB) at UCLA. Currently, he is an assistant professor of the Department of Engineering Science and Ocean Engineering at National Taiwan

University, Taipei, Taiwan. Prof. Chang founded the Computational Biomedical Laboratory (CBEL), whose goal is to build computational bridges between engineering and medicine. His research interests include variational methods for image restoration, registration and segmentation, computational biology and radiology, biomechanics modeling and biosystem simulation, pattern analysis and computer graphics, as well as medical informatics for healthcare applications.